GSK-3β in mouse fibroblasts controls wound healing and fibrosis through an endothelin-1–dependent mechanism

Mohit Kapoor,[1] Shangxi Liu,[1] Xu Shi-wen,[2] Kun Huh,[1] Matthew McCann,[1] Christopher P. Denton,[2] James R. Woodgett,[3] David J. Abraham,[2] and Andrew Leask[1]

[1]Division of Oral Biology and Department of Physiology and Pharmacology, University of Western Ontario, London, Ontario, Canada. [2]Centre for Rheumatology, University College London, London, United Kingdom. [3]Samuel Lunenfeld Research Institute, Mount Sinai Hospital, Toronto, Ontario, Canada.

Glycogen synthase kinase–3 (GSK-3) is a widely expressed and highly conserved serine/threonine protein kinase encoded by 2 genes, *GSK3A* and *GSK3B*. GSK-3 is thought to be involved in tissue repair and fibrogenesis, but its role in these processes is currently unknown. To investigate the function of GSK-3β in fibroblasts, we generated mice harboring a fibroblast-specific deletion of *Gsk3b* and evaluated their wound-healing and fibrogenic responses. We have shown that *Gsk3b*-conditional-KO mice (*Gsk3b*-CKO mice) exhibited accelerated wound closure, increased fibrogenesis, and excessive scarring compared with control mice. In addition, *Gsk3b*-CKO mice showed elevated collagen production, decreased cell apoptosis, elevated levels of profibrotic α-SMA, and increased myofibroblast formation during wound healing. In cultured *Gsk3b*-CKO fibroblasts, adhesion, spreading, migration, and contraction were enhanced. Both *Gsk3b*-CKO mice and fibroblasts showed elevated expression and production of endothelin-1 (ET-1) compared with control mice and cells. Antagonizing ET-1 reversed the phenotype of *Gsk3b*-CKO fibroblasts and mice. Thus, GSK-3β appears to control the progression of wound healing and fibrosis by modulating ET-1 levels. These results suggest that targeting the GSK-3β pathway or ET-1 may be of benefit in controlling tissue repair and fibrogenic responses in vivo.

Introduction

During tissue repair, which requires the reconstitution of the epithelial barrier and the underlying connective tissue (1), mesenchymal cells such as fibroblasts migrate into the wound area, where they create a new collagen- and cellular fibronectin–rich ECM (2). The specialized fibroblasts that perform this function are termed myofibroblasts, so called as they express the highly contractile protein α-SMA. Myofibroblasts generate the adhesive and tensile forces required for wound closure (3). During normal tissue repair, myofibroblasts disappear from the wound; persistence of the myofibroblast characterizes fibroproliferative diseases (3, 4), which affect the skin and internal organs, often resulting in organ failure and death. There is no therapy for fibrotic disease, as the fundamental mechanism underlying the progression from normal tissue repair to fibrogenesis is largely unknown.

Glycogen synthase kinase–3 (GSK-3), a widely expressed and highly conserved serine/threonine protein kinase, is encoded by 2 genes in mammals, generating GSK-3α and GSK-3β (5). GSK-3 was first isolated based on its activity on glycogen synthase but has broader roles in many cellular processes (6). The protein kinase is unusual, as it is generally highly active in resting cells but inhibited in response to cellular signals. These include signals activating receptor tyrosine kinases that activate the PI3K/PKB (Akt) pathway (7). GSK-3 also is involved with the canonical Wnt pathway, which relies on β-catenin (8). When Wnts bind the frizzled (Fz) receptor and coreceptor lipoprotein receptor–related protein 5 or 6 (LRP5/6), a cascade of signaling events causes the phosphorylation and inactivation of GSK-3β. GSK-3β normally phosphorylates β-catenin on serine and threonine residues, causing β-catenin to be targeted for degradation (9, 10). β-Catenin then migrates into the nucleus to activate transcription (11). β-Catenin expression is elevated in mesenchymal cells during the proliferative phase of wound healing, and it is overexpressed in conditions of fibroblast hyperproliferation, such as fibromatosis and hyperplastic scars (12, 13). Overexpression of β-catenin in mice results in fibrotic tumors in vivo, and wounding of these mice results in hyperplastic scarring (13). It has been hypothesized that inactivity of GSK-3β may play a role in these processes (14); however, this hypothesis has yet to be tested. Moreover, the transcriptional targets of the GSK-3β/β-catenin cascade mediating its effects on tissue repair and fibrogenesis have yet to be identified.

Mice lacking GSK-3β die late in gestation due to liver apoptosis (15). To evaluate whether GSK-3β plays a role in particular tissues or in adults, such as in wound healing or fibrogenesis, conditional ablation of GSK-3β in vivo is required. To investigate the mechanism of GSK-3β action in fibroblasts in vivo, we conditionally deleted *Gsk3b* in fibroblasts and assessed the response of these mice and fibroblasts derived from them to wound healing and fibrogenic responses in vivo and in vitro. Our results show that GSK-3β normally acts as a brake to terminate tissue repair through its ability to block ET-1 production and are consistent with the notion that a failure to properly terminate tissue repair results in fibrosis.

Results

Generation of Gsk3b-conditional-KO mice. To generate mice with deletion of *Gsk3b* in fibroblasts, we crossed mice harboring a *Gsk3b* allele with a floxed (i.e., flanked by *loxP* sites) exon 2 (*Gsk3b*^{F}) with mice containing a CreER(T) recombinase gene located down-

Nonstandard abbreviations used: CKO, conditional KO; ET-1, endothelin-1; GSK-3, glycogen synthase kinase–3; PCNA, proliferating cell nuclear antigen.

Conflict of interest: The authors have declared that no conflict of interest exists.

Citation for this article: *J. Clin. Invest.* **118**:3279–3290 (2008). doi:10.1172/JCI35381.

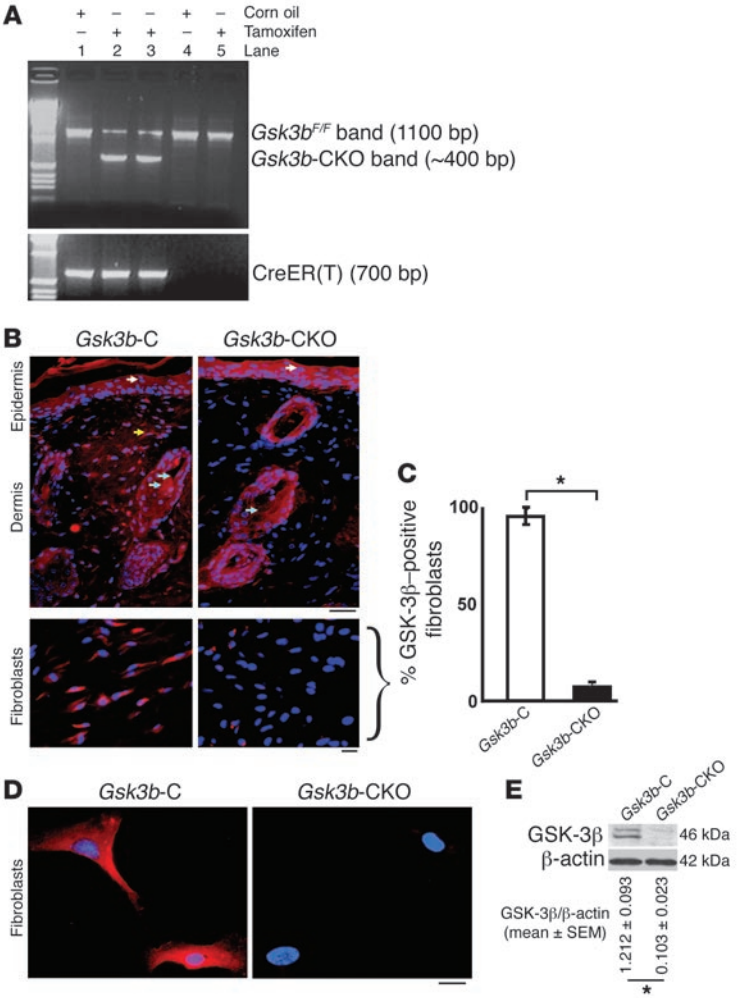

Figure 1
Conditional deletion of *Gsk3b* in fibroblasts. (**A**) PCR analysis of genomic DNA isolated from tails of Col1a2-creER(T)/0; *Gsk3b*$^{F/F}$ mice treated with corn oil (*Gsk3b*-C) or tamoxifen (*Gsk3b*-CKO) for 1 week. Col1a2-creER(T)/0; *Gsk3b*$^{F/F}$ mice treated with tamoxifen generated fibroblast-specific CKO mice. All genomic DNA samples were run on the same gel. Genotype of mice: lanes 1–3, Col1a2-creER(T)/0; *Gsk3b*$^{F/F}$ mice; lanes 4 and 5, *Gsk3b*$^{F/F}$ mice (**B**). GSK-3β immunofluorescence (in vivo). Immunofluorescence using GSK-3β antibody in day 0 unwounded skin of *Gsk3b*-C and *Gsk3b*-CKO mice. Scale bars: top row, 200 μm; bottom row, 100 μm. White arrows indicate GSK-3β–positive staining in the epidermis; yellow arrow, GSK-3β–positive staining in the dermis; blue arrows, GSK-3β–positive staining in hair follicles. Representative data from $n = 4$ animals per group are shown. (**C**) Percentage of GSK-3β–positive fibroblasts in *Gsk3b*-C versus *Gsk3b*-CKO mice. (**D**) GSK-3β immunofluorescence (in vitro). Immunofluorescence using GSK-3β antibody in dermal fibroblasts isolated from *Gsk3b*-C and -CKO mice. Representative data from $n = 8$ cell lines from 8 mice. Scale bar: 50 μm. (**E**) Loss of GSK-3β protein expression in fibroblasts isolated from *Gsk3b*-CKO mice. $n = 8$ cell lines from 8 mice is shown. $^*P < 0.05$.

stream of a proa2(I) collagen promoter/enhancer, which confers fibroblast-specific CreER(T) gene expression (16). The activation of CreER(T) is dependent on the presence of tamoxifen (16). Mice homozygous for the *Gsk3b*^{F} allele and hemizygous for the Col1α2-CreER(T) allele [Col1a2-cre-ER(T)/0; *Gsk3b*$^{F/F}$] were generated and treated with (to delete *Gsk3b*; *Gsk3b*-conditional-KO [*Gsk3b*-CKO] mice) or without tamoxifen (for controls; *Gsk3b*-C mice) as described in Methods. Deletion of the *Gsk3b* gene was verified using PCR analysis of tail DNA (Figure 1A). Immunofluorescence staining for GSK-3β in day 0 unwounded skins of *Gsk3b*-C and -CKO mice showed absence of GSK-3β expression only in fibroblasts, with no change in the staining profile in the epidermis and hair follicles of *Gsk3b*-CKO mice (Figure 1, B and C). Furthermore, immunofluorescence for GSK-3β in dermal fibroblasts showed absence of GSK-3β staining in *Gsk3b*-CKO fibroblasts compared with *Gsk3b*-C fibroblasts (Figure 1D). Loss of GSK-3β expression in *Gsk3b*-CKO fibroblasts was further confirmed by Western blot analyses using an anti–GSK-3β antibody (Figure 1E).

Conditional deletion of Gsk3b results in increased cutaneous wound repair, enhanced collagen synthesis, and decreased apoptosis, resulting in excessive scarring and fibrogenesis. To investigate whether *Gsk3b*-CKO mice displayed defects in cutaneous wound closure, we subjected 8-week-old *Gsk3b*-C and *Gsk3b*-CKO mice to the dermal punch wound model of wound healing. We monitored wound closure over a 10-day period and found that *Gsk3b*-CKO animals displayed a marked acceleration in wound closure relative to control animals (Figure 2, A and B). Histomorphometric examination of tissue sections from mice 7 days after wounding further revealed enhanced wound closure in *Gsk3b*-CKO mice (Figure 2, C and D). We conducted parallel studies with wild-type C57BL/6J mice treated with or without tamoxifen. Tamoxifen alone had no impact on wound closure (data not shown). Quantitative analysis of wound collagen synthesis using hydroxyproline assay showed enhanced collagen production in day 7 wound tissues of *Gsk3b*-CKO mice compared with control *Gsk3b*-C mice (Figure 3A). Seven days after wounding, *Gsk3b*-CKO animals showed enhanced α-SMA protein expression (Figure 3B) and elevated α-SMA–expressing myofibroblasts (Figure 3C). Day 7 wounds of *Gsk3b*-CKO mice showed increased cell proliferation as revealed by anti–proliferating cell nuclear antigen (anti-PCNA) antibody (Figure 3D). We then investigated the effect of conditional deletion of *Gsk3b* on apoptosis. Results showed decreased cell apoptosis in day 7 wounds of *Gsk3b*-CKO compared with *Gsk3b*-C mice, as revealed by Fluorescein FragEL DNA fragmentation assay (Figure 3E). Examination of animals 21 and 28 days after wounding revealed increased levels of collagen deposition and excessive scarring in *Gsk3b*-CKO mice as detected by van Gieson collagen stain (Figure 4A). Moreover, *Gsk3b*-CKO animals possessed an elevated maturity of collagen fibers (Figure 4B). In

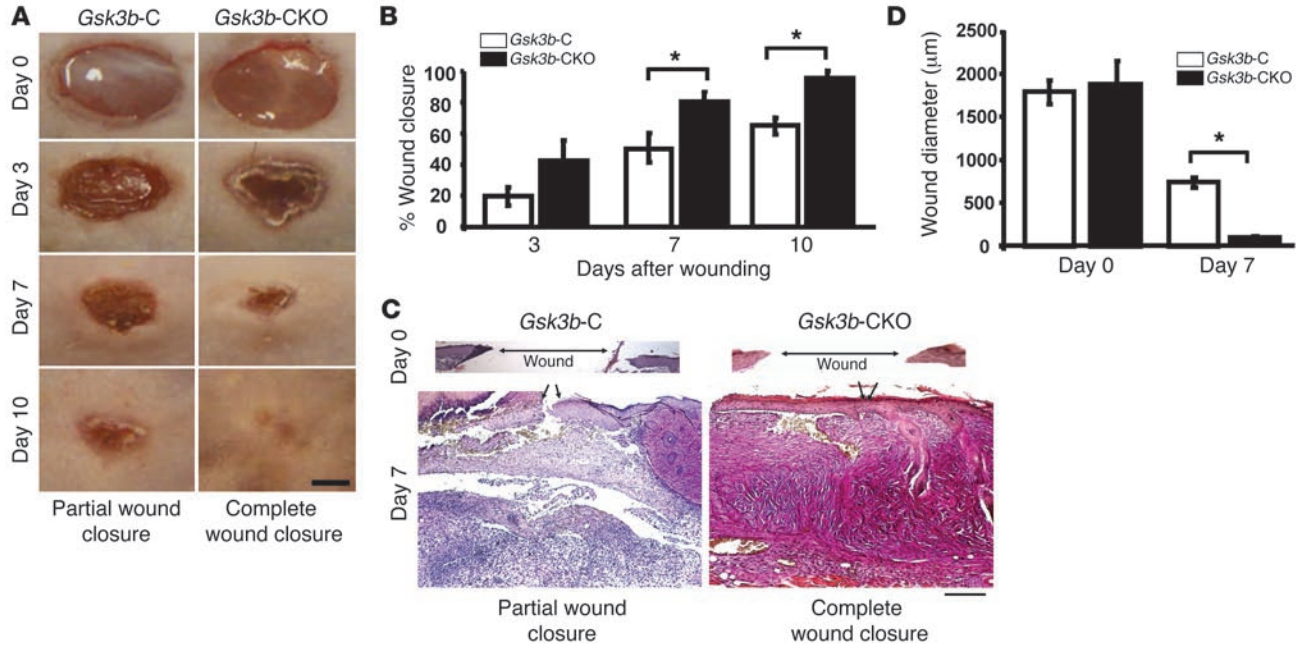

Figure 2

Loss of GSK-3β expression in fibroblasts results in enhanced wound closure. (**A** and **B**) Kinetics of wound closure. Microphotographs of wounds were captured on days 0, 3, 7, and 10 after wounding to determine the degree of wound closure in *Gsk3b*-CKO compared with *Gsk3b*-C mice. Total area of wounds at days 0, 3, and 7 after wounding was measured using Northern Eclipse software as described in Methods. *Gsk3b*-CKO mice showed a significant ($P < 0.05$) acceleration in wound closure compared with *Gsk3b*-C mice on days 7 and 10 after wounding. Representative data from $n = 8$ animals per group are shown. Scale bar: 1 mm. (**C** and **D**) Histomorphometric analysis of wound closure. Histomorphometric evaluation of wound closure was performed by measuring the diameter of day 0 and 7 wounds of *Gsk3b*-CKO versus *Gsk3b*-C mice. *Gsk3b*-CKO mice showed a significant ($P < 0.05$) decrease in wound diameter compared with *Gsk3b*-C mice on day 7 after wounding. Representative data from $n = 6$ animals per group are shown. Arrows indicate the leading edges of wounded epidermis. Scale bar: 200 μm. *$P < 0.05$.

addition, these animals had elevated hydroxyproline levels at day 21 after wounding, indicating increased collagen production persisting after wound closure, consistent with the development of fibrogenesis (Figure 4C). We also compared the thickness of wound epidermis (measured from basement membrane layer to the stratum corneum layer of the epidermis) on days 7, 21, and 28 after wounding in *Gsk3b*-C versus *Gsk3b*-CKO mice (Table 1). No significant differences in the epidermal thickness were observed in *Gsk3b*-C versus *Gsk3b*-CKO mice at each time point during wound healing.

Migration, spreading, adhesion, and contraction are elevated in GSK-3β–deficient fibroblasts. To further investigate the basis for the wound-healing phenotype of the *Gsk3b*-CKO animals, we explanted dermal fibroblasts from *Gsk3b*- and -CKO mice and subjected them to the scratch wound assay of in vitro repair. *Gsk3b*-CKO cells migrated faster than their counterparts (Figure 5, A and B). Cell spreading was monitored after adhesion microscopically, using rhodamine-phalloidin and anti-vinculin antibodies. We found that loss of GSK-3β also resulted in enhanced spreading of fibroblasts on fibronectin, as revealed with anti-vinculin antibody (green) and rhodamine-phalloidin (red) staining to detect actin (Figure 5C). To further investigate the contribution of GSK-3β to the function of fibroblasts, we assessed whether *Gsk3b*-CKO cells showed enhanced ability to adhere to fibronectin. We performed a standard quantitative adhesion assay, which showed increased *Gsk3b*-CKO cell adhesion to fibronectin (Figure 5D). Finally, *Gsk3b*-CKO cells had an elevated ability to contract a floating collagen gel matrix (Figure 5E).

α-SMA, collagen, and ET-1 expression is elevated in Gsk3b-CKO fibroblasts. The α-SMA–expressing myofibroblast is the cell type responsible for ECM remodeling in wound healing. Western blot analysis showed a significant increase ($P < 0.05$) in α-SMA protein expression in *Gsk3b*-CKO cells (Figure 6A). To investigate whether loss of GSK-3β showed any effect on myofibroblast formation, we used indirect immunofluorescence analysis with an anti–α-SMA antibody to show that *Gsk3b*-CKO cells had increased α-SMA expression and α-SMA–containing stress fibers (Figure 6B). Real-time PCR analysis also indicated elevated α-SMA and Col1a2 mRNA expression in *Gsk3b*-CKO cells (Figure 6C).

The vasoconstrictive protein endothelin-1 (ET-1) is elevated in fibrotic diseases such as scleroderma and is responsible for the persistent fibrotic phenotype of fibroblasts isolated from lesions of these patients (17–19). To investigate whether ET-1 may be playing a role in the phenotype of *Gsk3b*-CKO mice, we first showed elevated ET-1 protein expression in day 7 *Gsk3b*-CKO compared with *Gsk3b*-C wounds (Figure 7A). Immunohistochemistry showed enhanced ET-1–positive staining in day 7 wound tissues of *Gsk3b*-CKO compared with *Gsk3b*-C mice (Figure 7B). In isolated *Gsk3b*-CKO compared with *Gsk3b*-C fibroblasts, ET-1 mRNA and protein levels were elevated, as revealed by real-time PCR and a specific ET-1 ELISA, which detected secreted ET-1 in cell culture media (Figure 7, C and D).

ET-1 signaling is responsible for the Gsk3b-CKO phenotype. Based on these data, we hypothesized that ET-1 may be directly responsible for the phenotype of *Gsk3b*-CKO fibroblasts. We used the dual

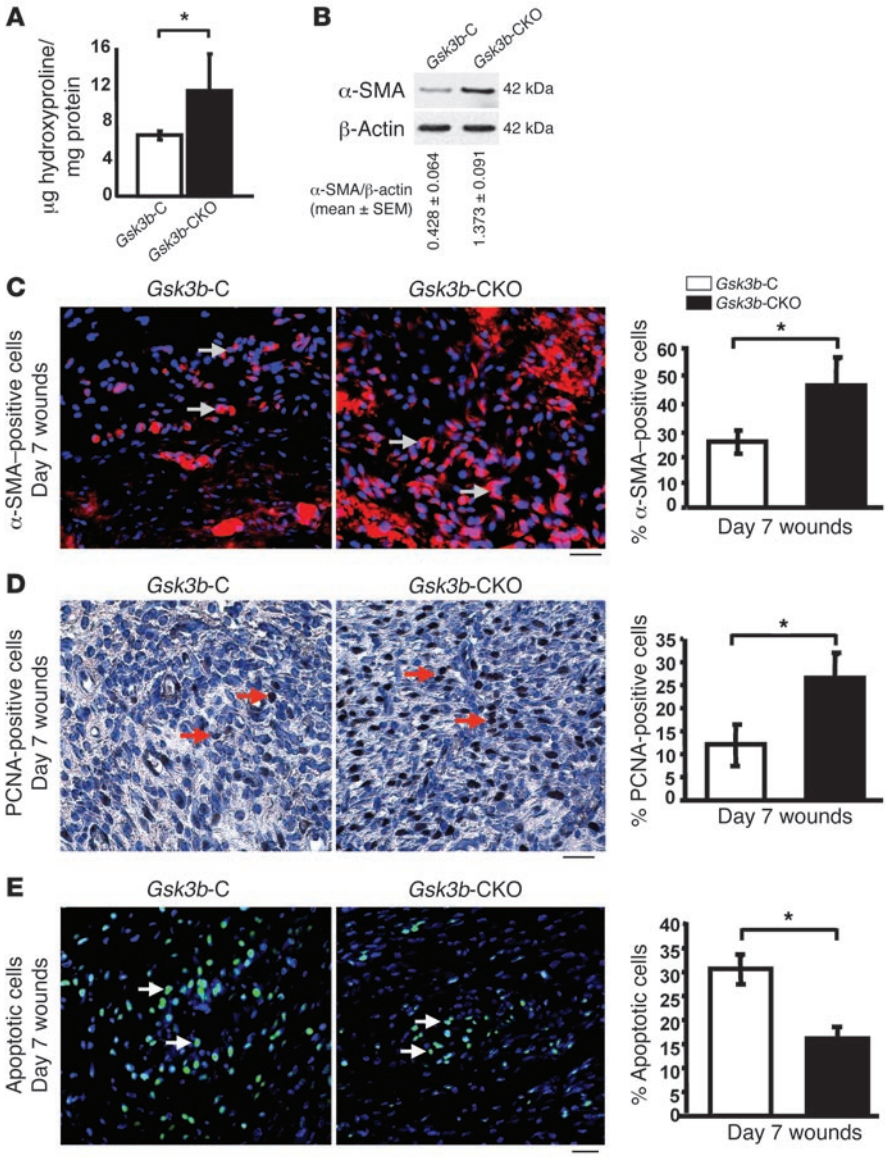

Figure 3
Conditional deletion of *Gsk3b* in fibroblasts results in elevated collagen, α-SMA production, and fibroblast proliferation and decreased apoptosis in vivo. (**A**) Wound collagen synthesis. Hydroxyproline levels (a marker of collagen synthesis) were assessed in day 7 wounds. Significantly ($P < 0.05$) higher levels of hydroxyproline were detected in day 7 wounds of *Gsk3b*-CKO mice compared with *Gsk3b*-C mice ($n = 6$ animals per group). (**B**) α-SMA protein expression. Western blot analysis showed a significant ($P < 0.05$) increase in the protein expression of α-SMA in day 7 wounds of *Gsk3b*-CKO compared with *Gsk3b*-C mice. Representative data from $n = 4$ animals per group are shown. (**C**) α-SMA staining. Immunofluorescence for α-SMA in day 7 wound sections showed a significant ($P < 0.05$) increase in the number of α-SMA–positive cells in *Gsk3b*-CKO compared with *Gsk3b*-C mice ($n = 6$ animals per group). Arrows indicate α-SMA–positive staining. Scale bar: 100 μm. (**D**) PCNA staining. Immunohistochemistry for PCNA in day 7 wound sections showed a significant ($P < 0.05$) increase in the number of PCNA-positive cells in *Gsk3b*-CKO compared with *Gsk3b*-C mice ($n = 4$ animals per group). Arrows indicate PCNA-positive staining. Scale bar: 100 μm. (**E**) Apoptosis assay in day 7 wound sections showed a significant ($P < 0.05$) decrease in the number of apoptotic cells in *Gsk3b*-CKO compared with *Gsk3b*-C mice ($n = 4$ animals per group). Arrows indicate apoptotic cells. Scale bar: 100 μm. *$P < 0.05$.

ETA/B receptor antagonist bosentan to assess whether the in vitro phenotype of *Gsk3b*-CKO fibroblasts was ET-1 dependent. We found that bosentan blocked the excess α-SMA stress fiber formation and protein expression (Figure 8, A and B), the overexpression of α-SMA and type I collagen mRNA (Figure 8, C and D), and the enhanced cell migration (Figure 8E), adhesion (Figure 8F), and ECM contraction of *Gsk3b*-CKO fibroblasts (Figure 8G). These results indicate that the in vitro fibrotic phenotype of *Gsk3b*-CKO fibroblasts was ET-1 dependent.

ETA/B receptor antagonism reverses the wound-healing and fibrotic phenotype of Gsk3b-CKO mice. Given that our previous analyses had uncovered that the in vitro fibrotic phenotype of *Gsk3b*-CKO fibroblasts was due to ET-1, we sought to assess whether the in vivo phenotype of *Gsk3b*-CKO mice was also due to ET-1. To investigate this question, mice were fed bosentan every day for 21 days. Bosentan had no effect on wound closure kinetics of normal control mice, indicating that ET-1 signaling did not play a role in normal wound healing. However, bosentan reversed the accelerated wound healing phenotype of *Gsk3b*-CKO mice (Figure 9, A and B). Moreover, bosentan reduced the collagen deposition and overexpression phenotype of *Gsk3b*-CKO mice (Figure 9, C and D) and reduced numbers of α-SMA–expressing myofibroblasts (Figure 9, E and F). In addition, bosentan rescued the loss of apoptosis in *Gsk3b*-CKO mice (Figure 9, G and H) These results indicate that ET-1 signaling contributes substantially to the altered wound repair responses resulting from the loss of GSK-3β but not appreciably to normal tissue repair. These results extend our in vitro analyses and suggest that the wound-healing and fibrotic phenotype of GSK-3β–deficient mice is due to elevated ET-1 production.

Overexpression of ET-1 in Gsk3b-CKO fibroblasts is due to elevated β-catenin expression. GSK-3β normally phosphorylates β-catenin on serine and threonine residues, causing β-catenin to be targeted for degradation. In the absence of GSK-3β, β-catenin escapes degradation and is translocated into the nucleus. We investigated whether loss of GSK-3β showed any effect on the expression of β-catenin in day 7 wounds of *Gsk3b*-CKO mice versus *Gsk3b*-C mice and in dermal fibroblasts isolated from *Gsk3b*-CKO mice versus *Gsk3b*-C mice. Results showed that loss of GSK-3β in fibro-

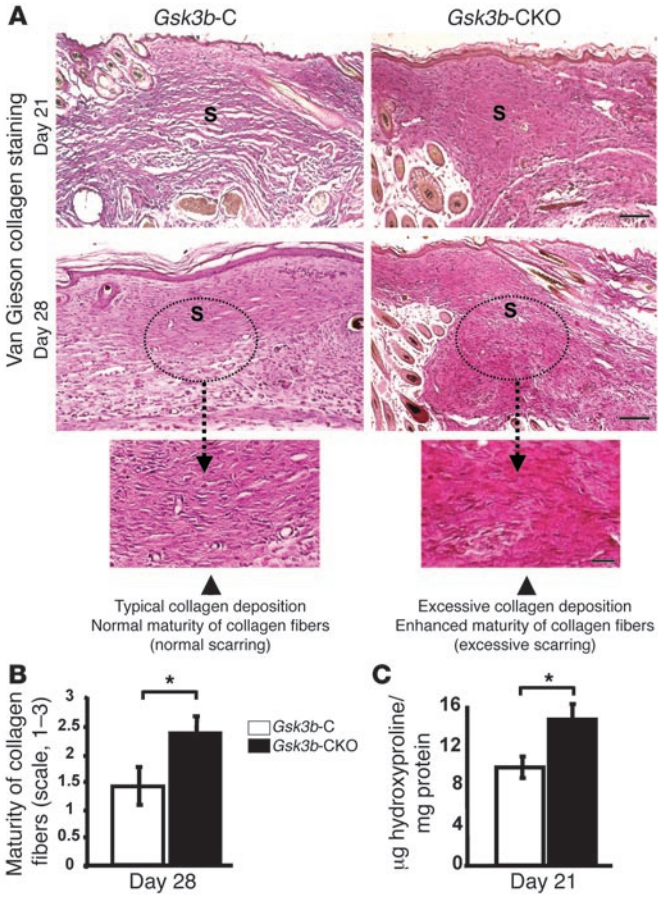

Figure 4
Conditional deletion of *Gsk3b* in fibroblasts results in excessive scarring during wound healing in vivo. (**A** and **B**) Quality of scarring. (**A**) Quality of scarring and collagen deposition was assessed by van Gieson collagen staining in day 21 and 28 wounds. A greater amount of collagen deposition in the dermis was observed in *Gsk3b*-CKO compared with *Gsk3b*-C mice on days 21 and 28 after wounding. By day 28 after wounding, *Gsk3b*-C mice exhibited a morphologically normal-looking scar, whereas *Gsk3b*-CKO mice exhibited excessive collagen deposition, with excessive scarring. Representative data from $n = 6$ animals per group are shown. Scale bars: top row, 200 μm; middle row, 200 μm; bottom row, 100 μm. (**B**) The van Gieson staining intensity was evaluated (see Methods) on the photomicrographs in a blinded manner and analysis performed on day 28. Van Gieson–stained wound sections showed more mature collagen fibers (deep red color of collagen fibers) in *Gsk3b*-CKO compared with *Gsk3b*-C mice (pink color of collagen fibers) ($n = 6$ animals per group). (**C**) Wound collagen synthesis. Significantly ($P < 0.05$) higher levels of hydroxyproline were detected in day 21 wounds of *Gsk3b*-CKO compared with *Gsk3b*-C mice ($n = 6$ animals per group). *$P < 0.05$. S, scar.

blasts resulted in enhanced protein expression of β-catenin in day 7 wounds of *Gsk3b*-CKO mice versus *Gsk3b*-C mice (Figure 10A). In addition, we observed enhanced β-catenin protein expression in *Gsk3b*-CKO versus *Gsk3b*-C fibroblasts (Figure 10B). Transfection with siRNA directed toward β-catenin, compared with control siRNA, showed that reduction in β-catenin expression decreased endothelin production in *Gsk3b*-CKO fibroblasts (Figure 10, C–E). These results indicate that loss of GSK-3β results in increased ET-1 production via elevated β-catenin expression, culminating in fibrogenesis (Figure 10F).

Discussion

In this study, we tested the effect of loss of GSK-3β in fibroblasts on tissue repair in vivo and in vitro. We performed this analysis using mice homozygous for a *Gsk3b* gene flanked by *loxP* sites and hemizygous for a transgene encoding a tamoxifen-dependent CreER(T) recombinase driven by a fibroblast-specific proα2(I) collagen promoter/enhancer (16). The tissue specificity of this promoter/enhancer construct has been confirmed in vivo (20). *Gsk3b*-CKO mice showed accelerated wound closure and enhanced collagen deposition. *Gsk3b*-CKO mice displayed decreased apoptosis and excessive tissue repair, resulting in excessive scarring and fibrogenesis in vivo. In addition, isolated *Gsk3b*-CKO fibroblasts showed increased myofibroblast formation, including elevated α-SMA expression and ECM contraction. The fibrogenic protein ET-1 (17–19) was overexpressed in *Gsk3b*-CKO mice in vivo and by *Gsk3b*-CKO fibroblasts in vitro. The phenotype of *Gsk3b*-CKO fibroblasts in vitro and *Gsk3b*-CKO mice in vivo was rescued by the dual ETA/B receptor antagonist bosentan. Of significance, ET receptor antagonism did not impede tissue repair in *Gsk3b*-C mice yet reverted the phenotype of *Gsk3b*-CKO mice to normal. These results suggest for the first time to our knowledge that loss of GSK-3β results in enhanced tissue repair and fibrogenesis in vivo, due to the elevated ET-1 levels.

Fibrotic diseases are characterized by the failure to terminate normal tissue repair and the persistence of myofibroblasts within lesions (4, 17, 19). A specific role for GSK-3β in wound healing is suggested by our finding that wound repair is severely enhanced

Table 1
Epidermal thickness of wounds in *Gsk3b*-C and *Gsk3b*-CKO mice

	Epidermal thickness (time course of wound healing)		
	Day 7	Day 21	Day 28
Gsk3b-C ($n = 6$)	69.81 ± 8.08	54.26 ± 5.29	44.43 ± 6.81
Gsk3b-CKO ($n = 5$)	79.22 ± 9.33	63.29 ± 11.01	48.99 ± 7.16

Epidermal thickness (measured from the basement membrane to the stratum corneum) of day 7, 21, and 28 wounds of *Gsk3b*-C and -CKO mice were measured using Northern Eclipse software. No significant changes in the epidermal thickness were observed on days 7, 21, and 28 after wounding in *Gsk3b*-C versus *Gsk3b*-CKO mice. Data represent epidermal thickness in micrometers. *n*, number of animals used at each time point/group.

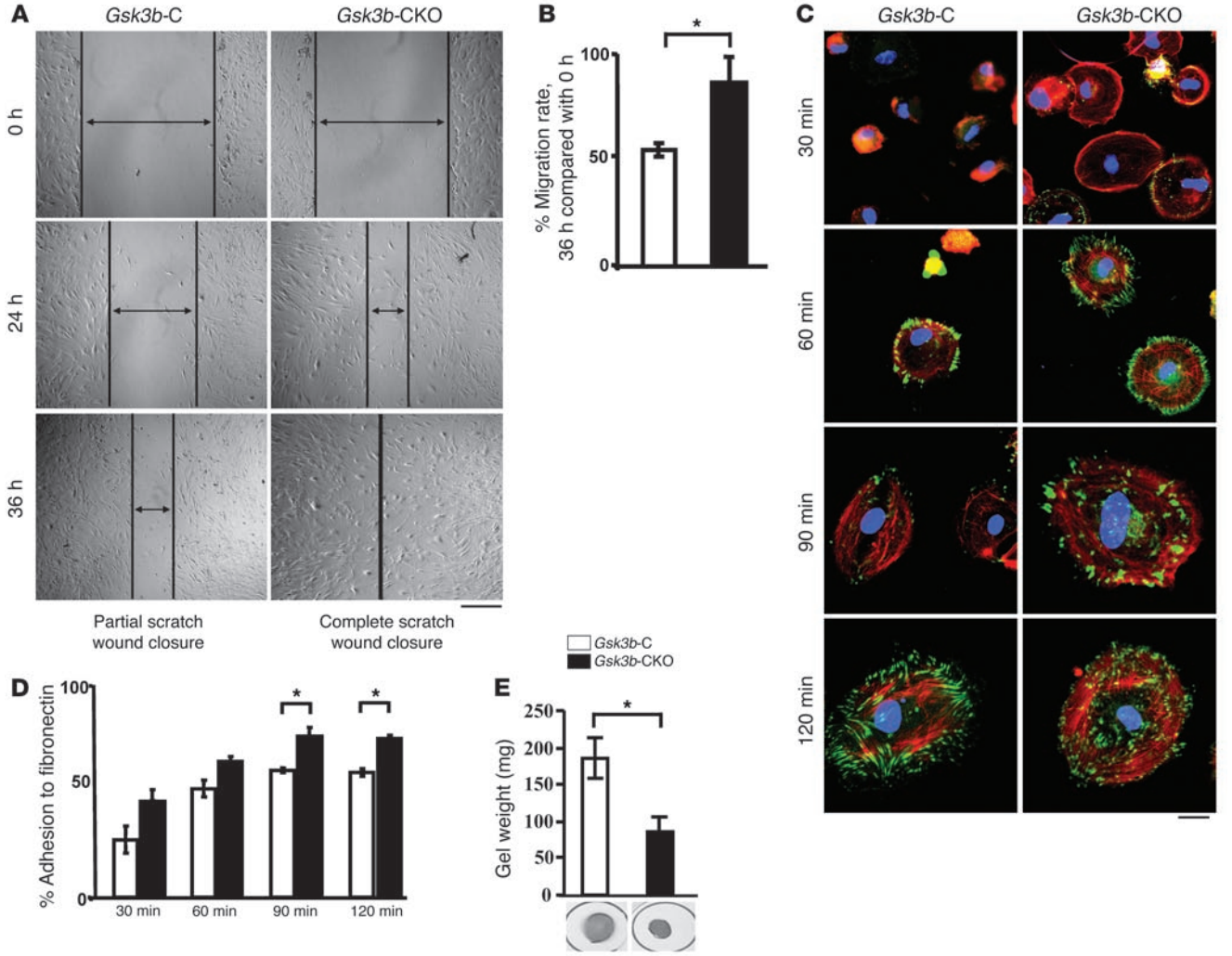

Figure 5

Loss of GSK-3β results in an enhanced ability of fibroblasts to migrate, spread, adhere, and contract on ECM in vitro. (**A** and **B**) Migration. Scratch assay was performed to assess the rate of migration of *Gsk3b*-C and *Gsk3b*-CKO dermal fibroblasts at 0, 24, and 36 hours after scratch injury. A significant ($P < 0.05$) increase in the migration rate was observed in *Gsk3b*-CKO compared with *Gsk3b*-C fibroblasts at 36 hours after scratch injury ($n = 4$ cell lines from 4 mice). Scale bar: 200 μm. (**C**) Cell spreading over fibronectin. Dermal fibroblasts were plated on fibronectin-coated plates for 30, 60, 90, and 120 minutes and stained with F-actin and vinculin. *Gsk3b*-CKO fibroblasts showed greater spreading over fibronectin compared with *Gsk3b*-C fibroblasts ($n = 4$ cell lines from 4 mice). Scale bar: 50 μm. (**D**) Percent adhesion to fibronectin. Dermal fibroblasts were plated on a 96-well plate coated with fibronectin and assessed for percent adhesion to fibronectin at 30, 60, 90, and 120 minutes by MTT assay. *Gsk3b*-CKO fibroblasts showed significantly greater adhesion to fibronectin compared with *Gsk3b*-C fibroblasts ($n = 4$ cell lines from 4 mice). (**E**) Contraction of collagen gel matrices. Loss of GSK-3β results in an enhanced ability of fibroblasts to contract a collagen gel matrix ($n = 4$ cell lines from 4 mice; mean ± SEM is indicated). *$P < 0.05$.

in mice carrying a dermis-specific deletion of *Gsk3b*. Moreover, our results indicate that loss of GSK-3β results in decreased cell apoptosis and excessive tissue repair, resulting in fibrogenesis through an ET-1–dependent mechanism. We have previously shown that overproduction of ET-1 by fibrotic fibroblasts is a key phenotypic feature of the disease systemic sclerosis, being responsible for the elevated α-SMA expression, adhesion, contraction, and migration of this cell type (17–19). Blockade of ET-1 action in these models did not appreciably affect normal cell physiology. Results presented here indicating that ET receptor antagonism suppressed the profibrotic effects of *Gsk3b* deletion without affecting the kinetics of the normal wound healing response emphasize that ET-1 appears to contribute to pathological wound-healing responses. Moreover, our data suggest that mutations or loss of function of GSK-3β may result in fibrotic conditions in vivo and that this effect may be mediated by ET-1. Our results showing that GSK-3β may function in vivo to suppress excessive tissue repair, and hence myofibroblast activity and fibrogenesis, provide a useful step in identifying the overall process underlying normal tissue repair and its progression to fibrogenesis. Finally, our results also strongly suggest that targeting GSK-3β or ET-1 may be an appropriate strategy for antifibrotic drug intervention.

ET-1 was identified more than 15 years ago as a small bioactive peptide derived from a larger peptide secreted from endothelial

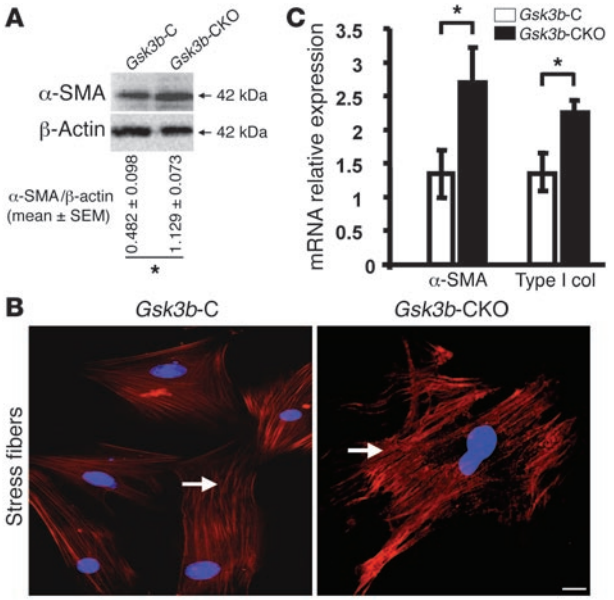

Figure 6
Loss of GSK-3β in fibroblasts results in increased α-SMA and type I collagen expression. (**A**–**C**) α-SMA and Col1a2 (type I collagen) expression. (**A**) α-SMA protein expression was assessed in *Gsk3b*-CKO versus *Gsk3b*-C dermal fibroblasts by Western blotting. *Gsk3b*-CKO fibroblasts showed significantly ($P < 0.05$) higher expression of α-SMA protein versus *Gsk3b*-C fibroblasts. Representative data from $n = 4$ cell lines from 4 mice are shown. (**B**) Immunofluorescence for α-SMA showed greater stress fiber formation and higher expression of α-SMA in *Gsk3b*-CKO versus *Gsk3b*-C fibroblasts ($n = 4$ cell lines from 4 mice). Arrows indicate α-SMA–positive stress fibers. Scale bar: 50 μm. (**C**) α-SMA and type I collagen mRNA expression was assessed in *Gsk3b*-CKO versus *Gsk3b*-C fibroblasts by real-time PCR. *Gsk3b*-CKO fibroblasts showed significantly ($P < 0.05$) higher expression of both α-SMA and type I collagen (Type I Col) protein versus *Gsk3b*-C fibroblasts ($n = 5$ cell lines from 5 mice). *$P < 0.05$.

cells (21). ET-1 has a potent vasoconstrictive role and, more recently, has been proposed to be a key contributor to pathological processes, including cancer and fibrosis (21, 22). Our data support a previously proposed notion that ET-1 is essential for driving the excessive scarring observed in fibrotic disease and, in particular, the lung fibrosis observed in scleroderma (17–19, 21, 22). Loss of GSK-3β results in activation of the β-catenin/Wnt signaling cascade, and previous data revealing that ET-1 is a direct target of Wnt signaling in NIH 3T3 fibroblasts (23) and that β-catenin induces ET-1 in colon cancer cells (24) are therefore consistent with the observations presented in this report. Nonetheless, our data indicate, we believe for the first time, (a) that loss of GSK-3β in fibroblasts results in excessive tissue repair and fibrosis and (b) that this is due to an elevation of ET-1. To our knowledge, ET-1 expression has not been previously demonstrated to impact GSK-3β.

In summary, our studies examining the involvement in GSK-3β in dermal function may have profound implications for both homeostatic and pathological wound-healing processes by contributing to our understanding of basic mechanisms regarding wound healing and its progression to fibrogenesis. Our results may therefore have long-term therapeutic implications for the treatment of nonhealing or chronic skin wounds and of fibrosis.

Methods

Generation of Gsk3b-CKO mice. The generation of mice expressing a conditional allele of GSK-3β was previously described (25). Briefly, R1 embryonic stem cells were electroporated with a modified GSK-3β targeting vector in which *loxP* sites were introduced in flanking exon 2 of GSK-3β. ES cell clones that had undergone correct homologous recombination were identified by Southern blot analysis and microinjected into C57BL/6J

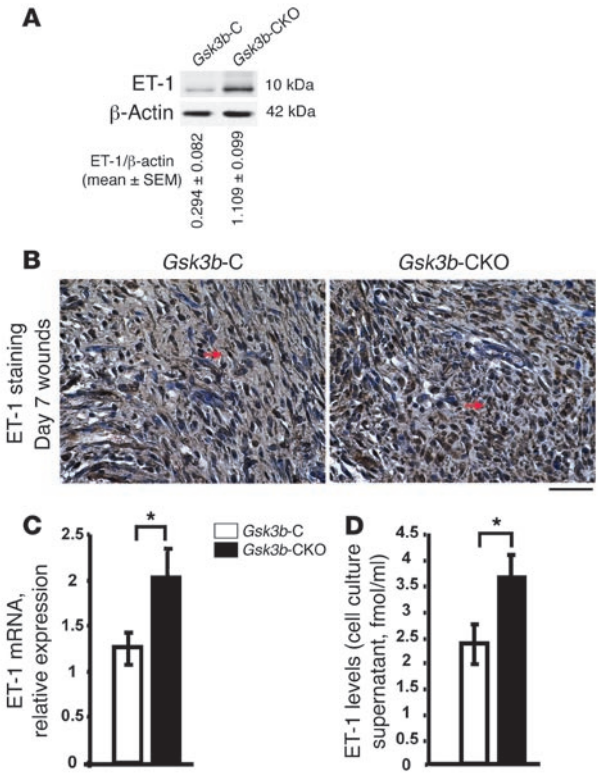

Figure 7
Loss of GSK-3β results in increased ET-1 expression. (**A**) ET-1 protein expression. Western blot analysis showed a significant ($P < 0.05$) increase in the protein expression of ET-1 in day 7 wounds of *Gsk3b*-CKO compared with *Gsk3b*-C mice. Representative data for $n = 8$ animals per group are shown. (**B**) ET-1 immunohistochemistry. Higher expression levels of ET-1 were detected in day 7 wounds of *Gsk3b*-CKO compared with *Gsk3b*-C mice. Representative data for $n = 4$ animals per group are shown. Arrows indicate ET-1–positive staining. Scale bar: 100 μm. (**C**) ET-1 mRNA expression was assessed in *Gsk3b*-CKO versus *Gsk3b*-C fibroblasts by real-time PCR. *Gsk3b*-CKO fibroblasts showed significantly ($P < 0.05$) higher expression of ET-1 mRNA versus *Gsk3b*-C fibroblasts ($n = 4$ cell lines from 4 mice). (**D**) ET-1 ELISA. ET-1 levels were assessed in the cell culture supernatants of *Gsk3b*-CKO versus *Gsk3b*-C fibroblasts by ELISA. *Gsk3b*-CKO fibroblasts showed significantly ($P < 0.05$) higher levels of ET-1 versus *Gsk3b*-C fibroblasts ($n = 6$ cell lines from 6 mice). *$P < 0.05$.

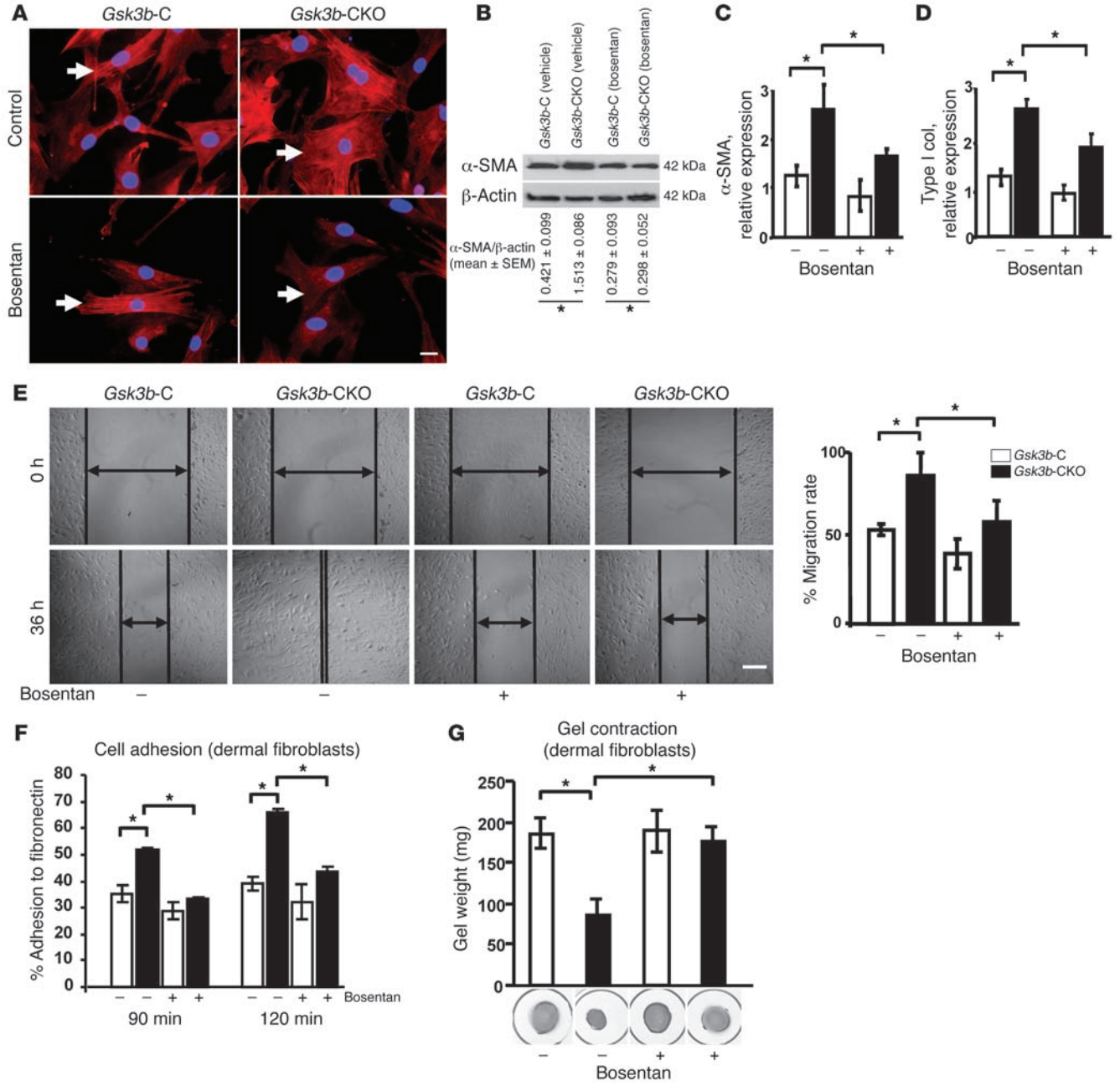

Figure 8

The dual ETA/B receptor antagonist bosentan alleviates the phenotype of GSK-3β–deficient fibroblasts (in vitro). (**A**) α-SMA immunofluorescence. *Gsk3b*-C and *Gsk3b*-CKO fibroblasts were treated with bosentan for 48 hours, and α-SMA immunofluorescence was performed. Representative data from $n = 4$ cell lines from 4 mice are shown. Arrows indicate α-SMA–positive stress fibers. Scale bar: 50 μm. (**B**) α-SMA protein expression. Bosentan treatment significantly ($P < 0.05$) reversed the enhanced protein expression of α-SMA in *Gsk3b*-CKO fibroblasts. Representative data from $n = 4$ cell lines from 4 mice are shown. (**C** and **D**) α-SMA and Col1a2 mRNA expression. Bosentan treatment significantly ($P < 0.05$) reduced the expression of both α-SMA and type I collagen in *Gsk3b*-CKO fibroblasts ($n = 5$ cell lines from 5 mice). (**E**) Migration scratch assay. Bosentan treatment significantly ($P < 0.05$) decreased migration of *Gsk3b*-CKO fibroblasts ($n = 4$ cell lines from 4 mice). Scale bar: 200 μm. (**F**) Percent adhesion to fibronectin. Bosentan treatment significantly ($P < 0.05$) reversed the enhanced adhesion of *Gsk3b*-CKO dermal fibroblasts to fibronectin ($n = 4$ cell lines from 4 mice). (**G**) Gel contraction assay. Bosentan treatment significantly ($P < 0.05$) reversed the enhanced ability of *Gsk3b*-CKO fibroblasts to contract the collagen gel matrix ($n = 3$; mean ± SEM is indicated). *$P < 0.05$.

blastocysts. The resultant chimeric mice were crossed to C57BL/6J (The Jackson Laboratory). Germline transmission of the *Gsk3b* floxed allele was verified by PCR. Interbreeding of these mice yielded *Gsk3b* floxed (*Gsk3b*$^{F/F}$) mice that were viable, healthy, born at the expected Mendelian frequency, and expressed GSK-3β at levels indistinguishable from those of wild-type animals.

C57BL/6J mice that carry a tamoxifen-inducible Cre-recombinase [CreER(T)] under the control of a fibroblast-specific regulatory sequence

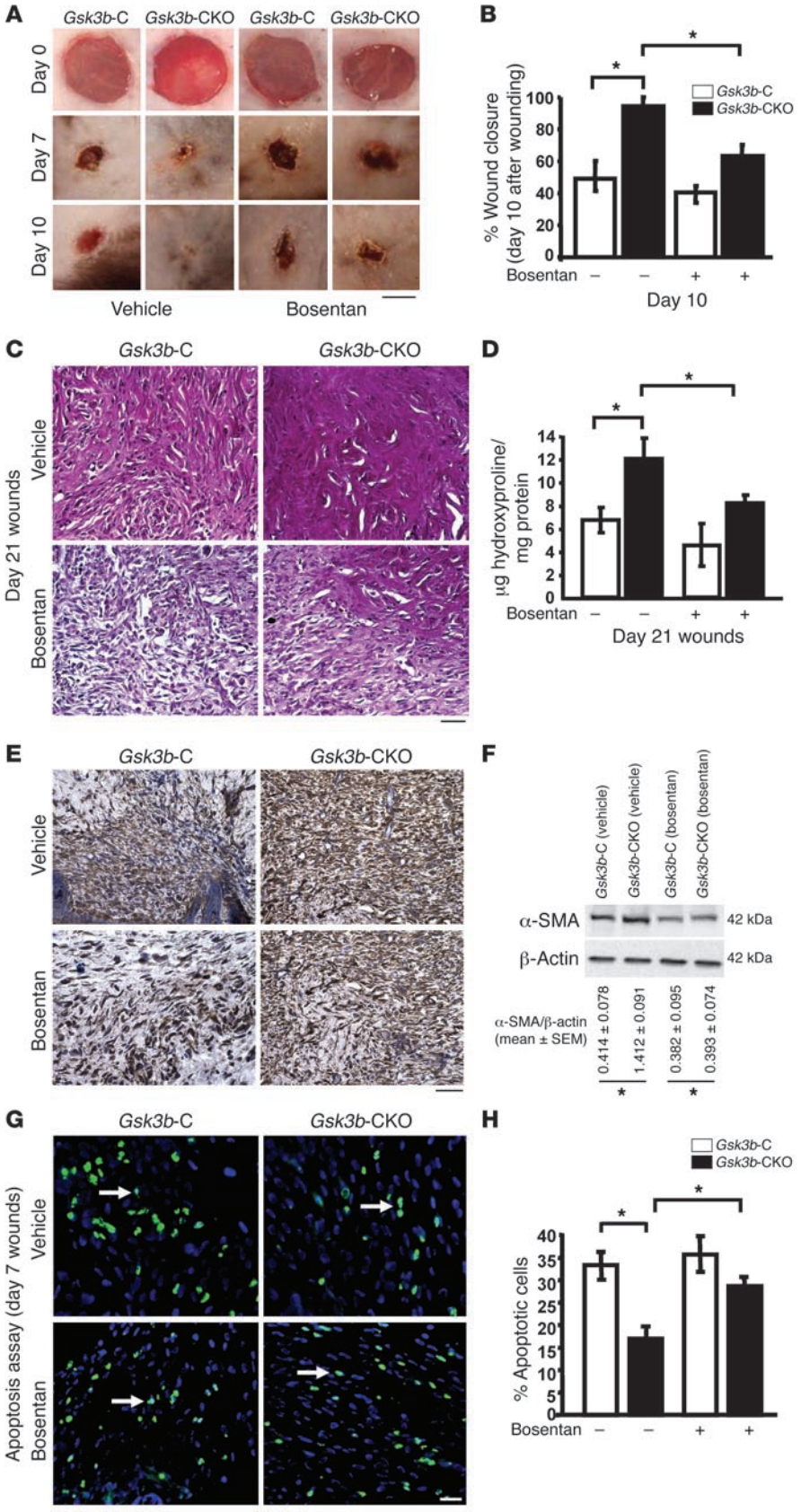

Figure 9

The dual ETA/B receptor antagonist bosentan alleviates the phenotype of GSK-3β–deficient mice (in vivo). (**A** and **B**) Kinetics of wound closure was determined in *Gsk3b*-C and *Gsk3b*-CKO mice treated with bosentan (100 mg/kg) or gum arabic (vehicle) on days 0, 7, and 10 after wounding. Bosentan treatment significantly ($P < 0.05$) reversed the enhanced rate of wound closure in *Gsk3b*-CKO mice without affecting the wound closure of *Gsk3b*-C mice ($n = 4$ wounds from 4 mice). Scale bar: 1 mm. (**C**) Effect of bosentan treatment on collagen synthesis was assessed using van Gieson staining in day 21 wounds. Note the reduction in the intensity of pink/red staining in *Gsk3b*-CKO animals in the presence of bosentan. Representative data from $n = 4$ wounds from 4 mice are shown. Scale bar: 100 μm. (**D**) Hydroxyproline levels. Bosentan ($P < 0.05$) reversed elevated wound collagen (hydroxyproline) synthesis in *Gsk3b*-CKO mice on day 21 after wounding ($n = 4$ wounds from 4 mice). (**E**) Bosentan ($P < 0.05$) reduced and reversed elevated α-SMA expression in *Gsk3b*-CKO mice on day 21 after wounding ($n = 4$ wounds from 4 mice). Scale bar: 100 μm. (**F**) Bosentan significantly ($P < 0.05$) reduced and reversed elevated α-SMA protein expression in *Gsk3b*-CKO mice on day 21 after wounding ($n = 3$). *$P < 0.05$. (**G** and **H**) Bosentan ($P < 0.05$) rescued loss of apoptosis in *Gsk3b*-CKO mice on day 7 after wounding ($n = 4$ wounds from 4 mice). Arrows indicate apoptotic cells. Scale bar: 100 μm. *$P < 0.05$.

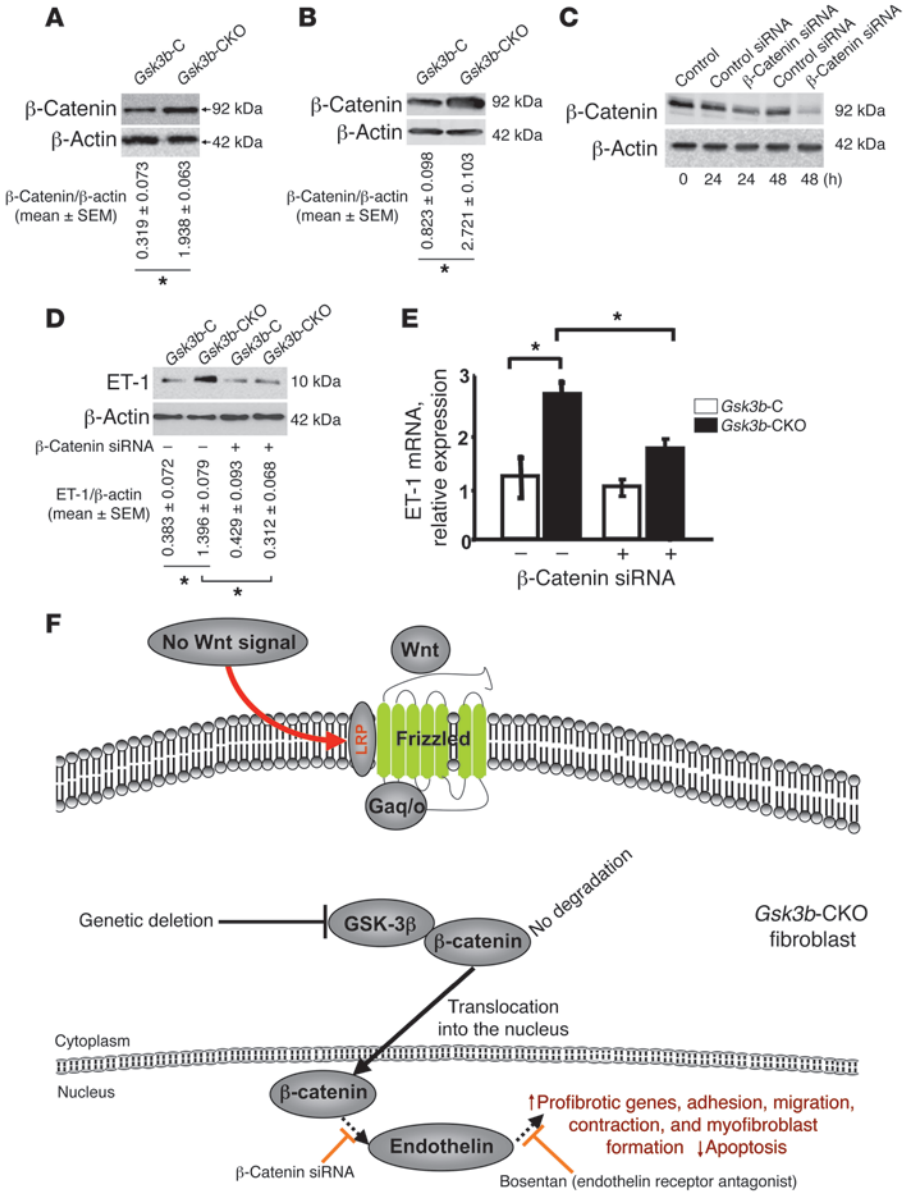

Figure 10
Loss of GSK-3β results in increased β-catenin, which is responsible for ET-1 overexpression. (**A** and **B**) β-Catenin protein expression. Western blot analysis showed a significant ($P < 0.05$) increase in the expression of β-catenin in day 7 wounds and dermal fibroblasts of *Gsk3b*-CKO compared with GSK-3β C mice. Representative data for $n = 4$ animals per group are shown. (**C**) siRNA recognizing β-catenin reduces β-catenin protein expression in *Gsk3b*-CKO fibroblasts. Transfection of *Gsk3b*-CKO fibroblasts with siRNA recognizing β-catenin, compared with control siRNA, reduced the expression of β-catenin as revealed by Western blot analysis with anti–β-catenin antibody. Hours after transfection are indicated. (**D** and **E**) siRNA recognizing β-catenin reduces ET-1 protein and mRNA expression in *Gsk3b*-CKO fibroblasts. Forty-eight hours after transfection with control or β-catenin siRNA, *Gsk3b*-CKO fibroblasts were examined for ET-1 protein production by Western blot analysis with anti–ET-1 antibody or by real-time PCR to detect ET-1 mRNA. Fibroblasts from 6 mice were used. *$P < 0.05$. (**F**) Model showing effect of loss of GSK-3β expression on tissue repair in vivo.

from the proα2(I) collagen gene [C57BL/6J-Tg(COL1a2-CreER(T))] (16) were crossed with *Gsk3b*$^{F/F}$ mice to generate mice heterozygous for both alleles. The second cross between *Gsk3b*$^{F/F}$ mice and heterozygous mice from the first cross produced Col1a2-CreER(T)/0; *Gsk3b*$^{F/F}$ mice, which were used for further experiments. Animals used for experiments were genotyped by PCR to detect GSK-3β and CreER(T) as described previously (5, 25). All animal protocols were approved by the regulatory authority of the Animal Use Subcommittee of the Council on Animal Care of the University of Western Ontario. To delete *Gsk3b*, a stock solution of tamoxifen (4-hydroxitamoxifen; Sigma-Aldrich) in ethanol (100 mg/ml) was diluted in corn oil to 10 mg/ml. Adult mice (age, 3 weeks) were given intraperitoneal injections of the tamoxifen suspension (0.1 ml of 10 mg/ml) over 10 days. Deletion of *Gsk3b* was tested by PCR genotyping using the following primers: forward, 5′-GGGGCAACCTTAATTTCATT-3′ and reverse, 5′-TCTGGGCTATAGCTATCTAGTAACG-3′. For CreER(T), the following primers were used: forward, 5′-ATCCGAAAAGAAAACGTTGA-3′ and reverse, 5′-ATCCAGGTTACGGATATAGT-3′. Deletion of GSK-3β was further confirmed by both immunofluorescence (both in vitro and in vivo) and Western blotting using an anti–GSK-3β antibody (Cell Signaling Technology).

Wound surgery. Experiments were performed on littermate mice homozygous for the *GSK-3β*^{F} (*loxP*–GSK-3β) allele and hemizygous for Col1a2-creER(T) [Col1a2-creER(T)/0; *Gsk3b*$^{F/F}$] that were treated with either tamoxifen (conditional knockout *Gsk3b* [*Gsk3b*-CKO]) or corn oil (control *Gsk3b* [*Gsk3b*-C]) alone. Wounding experiments were carried out 2 weeks after the last injection of tamoxifen. Mice were anesthetized by intraperitoneal injection of 90 μg ketamine plus 10 μg xylazine/g, and their back skin was shaved, depilated with Nair hair removal spray (Church & Dwight Co.), and cleaned with alcohol. Using a sterile 4-mm biopsy punch, 4 bilateral full-thickness skin wounds were created on the dorsorostral back skin without injuring the underlying muscle. Wounds were separated by a minimum of 6 mm of uninjured skin. Wounds were photographed at 0, 3, 7, and 10 days after wounding using a Sony D-9 digital camera. Wound area was measured using Northern Eclipse (Empix) software, and percentage wound closure at each time point was derived by following formula: (1 – [current

wound size/initial wound size]) × 100. Mice were sacrificed by CO_2 euthanasia after 3, 7, 21, and 28 days after wounding. Wound tissue biopsies were collected for histology, immunohistochemistry, immunofluorescence, hydroxyproline assay, and biochemical analysis.

Cell culture, immunofluorescence, and Western blot analysis. Dermal fibroblasts were isolated from explants (4- to 6-week-old animals) as previously described (4). Cells were subjected to indirect immunofluorescence analysis as previously described (6, 12) using anti–α-SMA, rhodamine-phalloidin (Sigma-Aldrich), and anti-vinculin (Sigma-Aldrich) antibodies, followed by an appropriate secondary antibody (Jackson ImmunoResearch Laboratories Inc.), and photography (Zeiss Axiphot) using a digital camera (Empix). Alternatively, cells were lysed in 2% SDS, and proteins quantified (Pierce) and subjected to Western blot analysis as previously described (4, 17, 26). The following primary antibodies were used for Western blotting: anti–GSK-3β (Cell Signaling Technology), anti-PCNA (Abcam), anti–α-SMA (Sigma-Aldrich), anti–β-actin (Sigma-Aldrich), phalloidin (Cytoskeleton), anti-vinculin (Sigma-Aldrich), ET-1 (Peninsula Laboratories), and anti–β-catenin (Cell Signaling Technology).

Apoptosis assay. Wound tissue sections (0.5 μm) were cut using a microtome (Leica) and collected on Superfrost Plus slides (Fisher Scientific). Sections were then dewaxed in xylene and rehydrated by successive immersion in descending concentrations of alcohol. Morphological evaluation of cells undergoing apoptosis during wound healing in *Gsk3b*-C and -CKO mice was performed using Fluorescein FragEL DNA Fragmentation Detection Kit (Calbiochem). Assay was performed according to the manufacturer's recommendations. Detection and analysis of labeling was performed by fluorescence microscopy (Zeiss Axiophot).

Real-time PCR. Real-time PCR was performed essentially as previously described (26, 27). Cells were cultured until 80% confluence and serum starved for 24 hours. Total RNA was isolated (RNeasy; QIAGEN). The integrity of the RNA was verified by gel electrophoresis or Agilent bioanalyzer. Total RNA (25 ng) was reverse transcribed and amplified using TaqMan Assays-on-Demand (Applied Biosystems) in a 15-μl reaction volume containing 2 unlabeled primers and 6-carboxyfluoroscein–labeled TaqMan MGB probe. Samples were combined with One-Step MasterMix (Eurogentec). Amplified sequences were detected using the ABI Prism 7900 HT sequence detector (Applied Biosystems) according to the manufacturer's instructions. Triplicate samples were run, and expression values were standardized to values obtained with control 28S RNA primers using the ΔCt method. Statistical analysis was performed using Student's paired *t* test.

Adhesion, contraction, and migration assays. Adhesion and contraction experiments were performed as previously described (4, 17). For in vitro wounding (migration) experiments, cultured fibroblasts obtained from *Gsk3b*-C and -CKO mice were grown in 12-well plates. Medium was removed, and cells were rinsed once with serum-free medium plus 0.1% BSA and were cultured for 24 hours in serum-free medium plus 0.1% BSA. The monolayer was artificially injured by scratching across the plate with a blue pipette tip (approximately 1.3 mm in width). The wells were washed 2 times to remove detached cells or cell debris. The cells were then cultured in serum-free medium. Mitomycin C (10 μg/ml; Sigma-Aldrich) was always included in the media to prevent cell proliferation. After 24 and 48 hours, images of the scratched areas under each condition were photographed. Scratch wound area was measured using Northern Eclipse (Empix) software, and percentage of wound closure at each time point was derived by following formula: (1 – [current wound size/initial wound size]) × 100.

Semiquantitative histological assessment of quality of scarring. Wound tissue sections (0.5 μm) were cut using a microtome (Leica) and collected on Superfrost Plus slides (Fisher Scientific). Sections were then dewaxed in xylene and rehydrated by successive immersion in descending concentrations of alcohol. To assess the effects of *Gsk3b* conditional deletion on wound collagen synthesis and quality of scarring, van Gieson collagen stain was used. Van Gieson stain results in a deep red color for mature collagen fibers and a pink color for immature collagen fibers. Muscle and fibrin appear yellow with black nuclei. Maturity of collagen fibers was assessed in a blinded manner using the following assessment criteria: 0 signifies pale pink color of collagen fibers; 1, pink color of collagen fibers; 2, pink and red color of collagen fibers; 3, deep red color of collagen fibers (similar to the surrounding unwounded dermis fibers).

Immunohistochemistry. Sections were cut and processed as described above. Immunolabeling of PCNA, α-SMA, and ET-1 was performed using the DakoCytomation LSAB+ System-HRP kit. Immunohistochemical procedures were performed according to the manufacturer's recommendations. Briefly, endogenous peroxide was blocked using 0.5% H_2O_2 in methanol for 5 minutes. Sections were incubated with BSA (1%) in PBS for 1 hour to block nonspecific IgG binding, then incubated with primary antibody against PCNA (1:50), α-SMA (1:1,000; Sigma-Aldrich), and ET-1 (1:100; Peninsula Laboratories) in a humidified chamber, and left overnight at 4°C. Next, sections were incubated with biotinylated link for 30 minutes, followed by incubation with streptavidin for 30 minutes. The chromogen diaminobenzidine tetrahydrochloride (DAB) was then added, and after color had developed sufficiently, sections were counterstained with Harris's hematoxylin. For PCNA, α-SMA, and ET-1 immunostaining, the number of PCNA-, α-SMA–, and ET-1–positive cells was calculated, divided by total number of cells, and the results expressed as percentage positive cells.

Hydroxyproline assay. Hydroxyproline assay was performed as a marker of collagen synthesis in wound tissues using the method previously described (28). Wound tissues were homogenized in saline and hydrolyzed with 2N NaOH for 30 minutes at 120°C, which was followed by the determination of hydroxyproline by modification of the Neumann and Logan's reaction (29) using chloramine T and Ehrlich's reagent, using a hydroxyproline standard curve and measuring at 550 nm. Values were expressed as micrograms of hydroxyproline per milligram of protein.

Bosentan treatment (in vitro). To inhibit the effects of ET-1, *Gsk3b*-C and -CKO dermal fibroblasts were grown to confluence and serum starved for 24 hours and then treated with bosentan (an endothelin receptor antagonist; 10 μM) for 48 hours. The effect of bosentan on migration, adhesion, and the expression of α-SMA and Col1a2 in *Gsk3b*-C and -CKO fibroblasts was determined as described above in Methods.

Bosentan treatment (in vivo). *Gsk3b*-C and -CKO mice were treated with 100 mg/kg/d bosentan monohydrate (a kind gift from Actelion; dosage recommended by the manufacturer) or vehicle (gum arabic; Sigma-Aldrich) for 21 days after wounding via oral gavage. The effect of bosentan treatment on wound closure was determined by photographing wounds at 0, 3, 7, and 10 days after wounding using a Sony D-9 digital camera. Wound area was analyzed using Northern Eclipse (Empix) software, and wound closure was expressed as percentage of initial wound size as described above in Methods. At the end of the 21-day time course, mice were killed by CO_2 asphyxiation. Wound tissue biopsies were collected for histology, immunohistochemistry, hydroxyproline assay, and biochemical analysis.

ET-1 enzyme immunoassay. The levels of ET-1 in cell culture supernatants of dermal fibroblasts extracted from *Gsk3b*-C and -CKO mice were determined by Endothelin ELISA kit (Biomedica). The assay was performed according to the manufacturer's recommendation.

β-Catenin siRNA transfection. To silence β-catenin, *Gsk3b*-C and -CKO dermal fibroblasts were transfected with β-catenin siRNA (20 nM; Dharmacon, USA) or control siRNA SiGLO (20 nM; Dharmacon) using Altogen fibroblast transfection reagent (Altogen Biosystems), and the manufacturer's recommended fibroblast transfection protocol was followed. The cells were grown for 48 hours after siRNA transfection, and efficacy of

β-catenin siRNA was assessed by Western blotting. The effect of β-catenin siRNA on the expression of ET-1 was then determined by real-time PCR and Western blotting.

Statistics. Statistical analysis was performed using 2-tailed Student's *t* test. Results are expressed as the mean ± SEM. $P < 0.05$ was considered statistically significant.

Acknowledgments

This work is supported by grants from the Canadian Foundation for Innovation and the Canadian Institutes of Health Research, the Arthritis Research Campaign, the Reynaud's and Scleroderma Foundation, and the Scleroderma Society. A. Leask is a New Investigator of the Arthritis Society (Scleroderma Society of Ontario), the recipient of an Early Researcher Award, and a member of the Canadian Scleroderma Research Group New Emerging Team. M. Kapoor is the recipient of postdoctoral fellowships from the Canadian Arthritis Network and the Ontario Ministry of Research and Innovation.

Received for publication February 19, 2008, and accepted in revised form August 13, 2008.

Address correspondence to: Andrew Leask, Canadian Institute of Health Research Group in Skeletal Development and Remodeling, Division of Oral Biology and Department of Physiology and Pharmacology, Schulich School of Medicine and Dentistry, University of Western Ontario, Dental Sciences Building, London, Ontario N6A 5C1, Canada. Phone: (519) 661-2111 ext. 81002; Fax: (519) 850-2459; E-mail: Andrew.leask@schulich.uwo.ca.

1. Martin, P. 1997. Wound healing — aiming for perfect skin regeneration. *Science.* **276**:75–81.
2. Eckes, B., Kessler, D., Aumailley, M., and Krieg, T. 1999. Interactions of fibroblasts with the extracellular matrix: implications for the understanding of fibrosis. *Springer Semin. Immunopathol.* **21**:415–429.
3. Gabbiani, G. 2003. The myofibroblast in wound healing and fibrocontractive diseases. *J. Pathol.* **200**:500–503.
4. Chen, Y., et al. 2005. Matrix contraction by dermal fibroblasts requires TGFbeta/ALK5, heparan sulfate containing proteoglycans and MEK/ERK: insights into pathological scarring in chronic fibrotic disease *Am. J. Pathol.* **167**:1699–1711.
5. Patel, S., Doble, B., and Woodgett, J.R. 2004. Glycogen synthase kinase-3 in insulin and Wnt signalling: a double-edged sword? *Biochem. Soc. Trans.* **32**:803–808.
6. Doble, B.W., and Woodgett, J.R. 2003. GSK-3: tricks of the trade for a multi-tasking kinase. *J. Cell Sci.* **116**:1175–1186.
7. Mitsiades, C.S., Mitsiades, N., and Koutsilieris, M. 2004. The Akt pathway: molecular targets for anticancer drug development. *Curr. Cancer Drug Targets.* **4**:235–256.
8. Nelson, W.J., and Nusse, R. 2004. Convergence of Wnt, beta-catenin, and cadherin pathways. *Science.* **303**:1483–1487.
9. Aberle, H., Bauer, A., Stappert, J., Kispert, A., and Kemler, R. 1997. beta-catenin is a target for the ubiquitin-proteasome pathway. *EMBO J.* **16**:3797–3804.
10. Orford, K., Crockett, C., Jensen, J.P., Weissman, A.M., and Byers, S.W. 1997. Serine phosphorylation-regulated ubiquitination and degradation of beta-catenin. *J. Biol. Chem.* **272**:24735–24738.
11. Behrens, J., et al. 1996. Functional interaction of beta-catenin with the transcription factor LEF-1. *Nature.* **382**:638–642.
12. Alman, B.A., Li, C., Pajerski, M.E., Diaz-Cano, S., and Wolfe, H.J. 1997. Increased beta-catenin protein and somatic APC mutations in sporadic aggressive fibromatoses (desmoid tumors). *Am. J. Pathol.* **151**:329–334.
13. Cheon, S.S., et al. 2002. beta-Catenin stabilization dysregulates mesenchymal cell proliferation, motility, and invasiveness and causes aggressive fibromatosis and hyperplastic cutaneous wounds. *Proc. Natl. Acad. Sci. U. S. A.* **99**:6973–6978.
14. Cheon, S., et al. 2005. Prolonged beta-catenin stabilization and tcf-dependent transcriptional activation in hyperplastic cutaneous wounds. *Lab. Invest.* **85**:416–425.
15. Hoeflich, K.P., et al. 2000. Requirement for glycogen synthase kinase-3beta in cell survival and NF-kappaB activation. *Nature.* **406**:86–90.
16. Zheng, B., Zhang, Z., Black, C.M., de Crombrugghe, B., and Denton, C.P. 2002. Ligand-dependent genetic recombination in fibroblasts: a potentially powerful technique for investigating gene function in fibrosis. *Am. J. Pathol.* **160**:1609–1617.
17. Shi-Wen, X., et al. 2004. Endothelin-1 promotes myofibroblast induction through the ETA receptor via a rac/phosphoinositide 3-kinase/Akt-dependent pathway and is essential for the enhanced contractile phenotype of fibrotic fibroblasts. *Mol. Biol. Cell.* **15**:2707–2719.
18. Shi-wen, X., et al. 2006. Constitutive ALK5-independent JNK activation contributes to endothelin-1 over-expression in pulmonary fibrosis. *Mol. Cell. Biol.* **26**:5518–5527.
19. Shi-wen, X., et al. 2007. Endogenous endothelin-1 signaling contributes to Col1a2 and CCN2 overexpression in fibrotic fibroblasts. *Matrix Biol.* **26**:625–632.
20. Ponticos, M., et al. 2004. Col1a2 enhancer regulates collagen activity during development and in adult tissue repair. *Matrix Biol.* **22**:619–628.
21. Clozel, M., and Salloukh, H. 2005. Role of endothelin in fibrosis and anti-fibrotic potential of bosentan. *Ann. Med.* **37**:2–12.
22. Leask, A. 2008. Targeting the TGFβ, endothelin-1 and CCN2 axis to combat fibrosis in scleroderma. *Cell. Signal.* **20**:1409–1414.
23. Chen, S., McLean, S., Carter, D.E., and Leask, A. 2007. The gene expression profile induced by Wnt 3a in NIH 3T3 fibroblasts. *J. Cell. Commun. Signal.* **1**:175–183.
24. Kim, T.H., Xiong, H., Zhang, Z., and Ren, B. 2005. beta-Catenin activates the growth factor endothelin-1 in colon cancer cells. *Oncogene.* **24**:597–604.
25. Tanabe, K., et al. 2008. Genetic deficiency of glycogen synthase kinase-3beta corrects diabetes in mouse models of insulin resistance. *PLoS Biol.* **6**:e37.
26. Kennedy, L., et al. 2007. CCN2 is essential for fibroblast function. *Exp. Cell Res.* **313**:952–964.
27. Shi-wen, X., et al. 2006. CCN2 is necessary for adhesive responses to TGFβ1 in embryonic fibroblasts. *J. Biol. Chem.* **281**:10715–10726.
28. Reddy, G.K., and Enwemeka, C.S. 1996. A simplified method for the analysis of hydroxyproline in biological tissues. *Clin. Biochem.* **29**:225–229.
29. Neuman, R.E., and Logan, M.A. 1950. The determination of hydroxyproline. *J. Biol. Chem.* **184**:299–306.